**THE EUROPEAN
PHYSICAL JOURNAL D**

Regular article

Positron annihilation in large polyatomic molecules. The role of vibrational Feshbach resonances and binding

G.F. Gribakin[a] and C.M.R. Lee

Department of Applied Mathematics and Theoretical Physics, Queen's University, Belfast BT7 1NN, Northern Ireland, UK

Abstract. We analyse the process of rapid positron annihilation in large polyatomic molecules due to positron capture into vibrational Feshbach resonances. Resonant annihilation occurs in molecules which can bind positrons, and we analyse positron binding to alkanes using zero-range potentials. Related questions of spectra of annihilation gamma quanta and molecular fragmentation following annihilation, are discussed briefly.

PACS. 34.80.Uv Positron scattering – 78.70.Bj Positron annihilation – 71.60.+z Positron states – 34.80.Gs Molecular excitation and ionization

1 Introduction

In this paper we analyse the mechanisms of positron annihilation in large polyatomic molecules. We also discuss a number of related phenomena: positron binding, spectra of annihilation gamma quanta and molecular fragmentation induced by annihilation.

So far these studies have involved alkanes and other organic molecules and their substitutes but not biomolecules, such as proteins or DNA. However, the physics of positron annihilation in many large polyatomic molecules should have much in common. Positron annihilation in biological systems is at the heart of positron emission tomography (PET) [1]. In particular, PET is an essential tool for in situ beam observation and control of the dose in heavy-ion tumor therapy (see, e.g., [2]). Positron interactions with living tissue also form the basis of *positherapy* [3].

As we shall see, rapid positron annihilation in many polyatomics is due to a two-step process involving positron attachment to the molecule. This makes it similar to electron-molecule attachment procceses. Electron attachment leads to formation of transient negative ions states, which mediate and enhance molecular dissociation and vibrational excitation. They play a very important role in many gas-phase phenomena [4]. Low-energy dissociative electron attachment is also known to cause single-strand breaks in DNA [5]. There is a lot of similarity between the interactions of low-energy electrons and positrons with atoms and molecules. This interaction is dominated by long-range polarisation attraction, and is capable of supporting bound states. In both cases, attachment is ac-

companied by excitation of the molecular nuclear motion. From this point of view, understanding positron annihilation sheds light on general features of low-energy attachment processes.

At the fundamental level, the positron is the simplest and most abundant piece of antimatter. It is the first antiparticle to ever have been discovered, first "at the tip of a pen" by Dirac, as a solution of the relativistic wave equation for the electron [6], and then experimentally in the cosmic rays by Anderson [7].

On the practical side, owing to their unique annihilation gamma quanta signal, positrons make an excellent probe. Besides their use in PET for studying structures and processes in living organisms, they find very wide application in various kinds of condensed phase spectroscopy. By studying positron lifetimes and spectra of annihilation gamma rays, one can obtain information about the shape of the Fermi surface, concentration and types of dopants or defects, porosity, phase transitions in microvoids, etc. By using positron beams of varying energy, one can probe surfaces and perform depth profiling [8]. Annihilation signal of 511 keV gamma rays also tells us about copious production of positrons near the centre of our galaxy [9].

To fully utilise the information contained in the annihilation gamma signal, one needs to understand the details of the positron annihilation process. The basic electron-positron annihilation event is described by quantum electrodynamics. In the non-relativistic Born approximation the annihilation cross section averaged over the directions of electron and positron spins, is given by (see, e.g., Ref. [10])

$$\overline{\sigma}_{2\gamma} = \pi r_0^2 \frac{c}{v}, \tag{1}$$

---

[a] e-mail: `g.gribakin@qub.ac.uk`

where v is their relative velocity, c is the speed of light, and r_0 is the classical electron radius defined by $e^2/r_0 = mc^2$, e and m being the electron charge and mass[1].

Estimating (1) and making use of atomic units (where $m = |e| = \hbar = 1$ and $c = \alpha^{-1} \approx 137$) we see that the annihilation cross section, $\overline{\sigma}_{2\gamma} \sim 10^{-8} c/v$ a.u., is small, even if the velocity is low, e.g., atomic-sized, $v \lesssim 1$ a.u., or thermal, $v \sim 0.05$ a.u. at room temperature. When a fast positron, e.g., that emitted in a β^+ radioactive decay with an energy of ~ 1 MeV, interacts with atomic matter, it undergoes a quick succession of inelastic collisions which have larger cross sections. It loses its energy, first due to ionisation, then electronic excitation, and then vibrational excitation in molecular media, or phonon emission in crystalline solids. As a result, the positron will typically slow down to eV or thermal energies (25 meV for $T = 300$ K) before annihilation.

In this work we are concerned with elementary annihilation events in binary encounters between the positron and an atom or molecule, such as those that take place in a gas. The low-energy positron annihilation rate in a gas, λ, is usually written in terms of a dimensionless parameter Z_{eff} [11], defined by

$$\lambda = \sigma_a v n \equiv \pi r_0^2 c n Z_{\text{eff}}, \tag{2}$$

where σ_a is the annihilation cross section, v is the positron velocity, and n is the number density of the gas. Comparing equations (1) and (2), we see that Z_{eff} can be interpreted as an *effective number of electrons* per atom or molecule, that contribute to annihilation.

Theoretically, Z_{eff} is given by the electron-positron contact density[2],

$$Z_{\text{eff}} = \int \sum_{i=1}^{Z} \delta(\mathbf{r} - \mathbf{r}_i)|\Psi_{\mathbf{k}}(\mathbf{r}_1, \ldots, \mathbf{r}_Z, \mathbf{r})|^2 d\mathbf{r}_1 \ldots d\mathbf{r}_Z d\mathbf{r}, \tag{3}$$

where $\mathbf{r}$ and $\mathbf{r}_i$ are the coordinates of the positron and ith electron, respectively, and $\Psi_{\mathbf{k}}(\mathbf{r}_1, \ldots, \mathbf{r}_Z, \mathbf{r})$ is the total wavefunction of the system, which describes scattering of the positron with initial momentum $\mathbf{k}$ from an atom or molecule. It is normalised to the incident positron plane wave, so that when the positron is outside the target, one has

$$\Psi_{\mathbf{k}}(\mathbf{r}_1, \ldots, \mathbf{r}_Z, \mathbf{r}) \simeq \Phi_0(\mathbf{r}_1, \ldots, \mathbf{r}_Z)\left[e^{i\mathbf{k}\cdot\mathbf{r}} + f_{\mathbf{k}\mathbf{k}'}\frac{e^{ikr}}{r}\right], \tag{4}$$

where Φ_0 is the initial target state (usually taken to be its ground state), and $f_{\mathbf{k}\mathbf{k}'}$ is the scattering amplitude for

---

[1] This cross section describes two-photon annihilation allowed when the total spin of the electron-positron pair, S, is zero. For $S = 1$ the electron and positron annihilate into three photons. The spin-averaged cross section of three-photon annihilation is 400 times smaller: $\overline{\sigma}_{3\gamma} = [4(\pi^2 - 9)/3]\alpha r_0^2 (c/v)$, where $\alpha = e^2/\hbar c \approx 1/137$ [10].

[2] In the nonrelativistic picture, annihilation takes place at a point, and the annihilation rate is proportional to the electron density at the positron, cf. calculation of the positronium (Ps) lifetime in [10].

Table 1. Annihilation parameter Z_{eff} at room temperature and estimated and measured positron binding energies $|\varepsilon_0|$ for alkanes.

Molecule	Z_{eff}	Binding energy (meV)	
		Est.[c]	Exp.[d]
CH_4	142^a	–	–
C_2H_6	660^b	–	$\gtrsim 0$
C_3H_8	$3\,500^b$	22	10
C_4H_{10}	$11\,300$	42	35
C_5H_{12}	$37\,800$	65	60
C_6H_{14}	$120\,000$	90	80
C_7H_{16}	$242\,000$	103	105
C_8H_{18}	$585\,000$	122	115
C_9H_{20}	$643\,000$	–	145
$C_{10}H_{22}$	$728\,000$	–	–
$C_{12}H_{26}$	$1\,780\,000$	–	220
$C_{16}H_{34}$	$2\,230\,000$	–	310

[a] Reference [16].
[b] Reference [15]; the rest are measurements in the positron trap [18].
[c] Values chosen to reproduce thermal Z_{eff} from equation (15).
[d] Obtained from the downshifts of the C–H mode resonances in Z_{eff} [19–22].

the final positron momentum $\mathbf{k}'$. In positron-molecule collisions, the wavefunction $\Psi_{\mathbf{k}}$ also depends on the nuclear coordinates, and they must be integrated over in equation (3).

Originally, Z_{eff} was introduced in an expectation that the annihilation rate would be comparable to the number of target electrons, Z. Indeed, if one neglects the interaction between the positron and the target and assumes that $\Psi_{\mathbf{k}}$ is equal to the right-hand side of equation (4) with $f_{\mathbf{k}\mathbf{k}'} = 0$, then equation (3) yields $Z_{\text{eff}} = Z$. However, early experiments [12–14] and later systematic studies [15–18] found that for many polyatomic molecules Z_{eff} exceeded Z by orders of magnitude. These measurements were done under equilibrium conditions with thermalised positrons, mostly at room temperature. They uncovered rapid growth of Z_{eff} with molecular size and very strong chemical sensitivity, as illustrated by Tables 1 and 2.

For the alkanes listed in Table 1, the number of electrons increases linearly with the molecular size, while Z_{eff} increases exponentially. On the other hand, when all the hydrogens in a molecule are replaced with fluorines (each of which has nine electrons), the molecular Z_{eff} actually drops! For example, $Z_{\text{eff}} = 54.4, 152, 317, 630$ and 1064 for perfluorinated molecules with $n = 1, 2, 3, 6$ and 8 carbon atoms, respectively. In contrast, heavier halogen substitutes increase the annihilation rate, e.g., $Z_{\text{eff}} = 9\,530$ for CCl_4, $39\,800$ for CBr_4, and $68\,600$ for C_2Cl_6. A comprehensive study by Iwata et al. [18] reported Z_{eff} data for many other small and large polyatomics, with the highest $Z_{\text{eff}} = 4.33 \times 10^6$ for antracene, $C_{14}H_{10}$, and 7.56×10^6 for the sebasic acid dimethyl ester, $C_{12}H_{22}O_4$.

A striking example of chemical sensitivity is provided by benzene and its derivatives. Here replacing a single

Table 2. Annihilation parameter Z_{eff} at room temperature for benzene C_6H_6 and substituted benzenes C_6H_5X, reference [18].

		Substituted atom or group X					
	C_6H_6	D	F	Cl	Br	CH_3	NO_2
$Z_{eff}/10^3$	15	36.9	34	72.3	172	190	430

hydrogen with another atom or a small group leads to great changes in Z_{eff}, Table 2. None of the effects illustrated by Tables 1 and 2 can be understood by regarding molecules as mere "clumps" of $Z_{eff} \sim Z$ electrons.

In spite of the gross discrepancy between experimental data and naïve view of Z_{eff}, the problem remained poorly understood for decades. Explanations of high molecular Z_{eff} were sought in terms of positron virtual or weakly bound states [23], resonances [24,25], or long-lived vibrationally excited positron-molecule complexes [17]. All of these have now become part of the comprehensive picture that is emerging thanks to a concerted effort from theory [26–28] and energy-resolved annihilation measurements [19–22]. In particular, these experiments yielded first direct evidence of positron-molecule binding which manifested itself through downshifts of the vibrational resonances. At the same time, calculations of positron-molecule annihilation, which neglected molecular vibrations, failed to reproduce "anomalous" Z_{eff} for polyatomics [29,30], but provided some indication that Z_{eff} might depend on the molecular geometry [31].

In this work we review the basic mechanisms of positron annihilation in molecules. In Section 2.2 we analyse the possible role of vibrationally inelastic positron escape in moderating the grown of Z_{eff} with molecular size. In Section 3 the role of vibrational mode-based doorway resonances is clarified, and an effective number of multimode vibrational resonances per doorway is estimated by comparison with experiment. Section 4 presents the results of improved modelling of positron binding to alkanes, including a close prediction of the second positron bound state. Finally, in Section 5 molecular fragmentation following annihilation is addressed. We propose that different positron localisation in the first and second bound states may lead to distinct molecular fragmentation patterns in these two cases.

2 Annihilation mechanisms

Positron annihilation in binary collisions can be understood in terms of two basic mechanisms, direct and resonant [26,27]. The first one operates for both atoms and molecules, and involves positron annihilation in flight, as it is passing the target. It is enhanced if the positron possesses a virtual of weakly bound level close to zero energy [23,32]. However, this enhancement is limited to $Z_{eff} \lesssim 10^3$ for room-temperature or higher positron energies (see Sect. 2.1).

Understanding the role and size of positron-atom attraction for noble-gas atoms [32,33] led to the discov-

ery that many neutral atoms support positron bound states [34,35]. This was a strong indicator that many molecules should also be capable of forming bound states with the positron[3]. Such binding gives rise to the resonant annihilation mechanism, in which the positron is temporarily captured into the bound state. During capture the positron transfers its excess energy (kinetic + binding) into the vibrational motion of the molecule, forming vibrational Feshbach resonances (VFR). For the capture to be effective, this energy must lie in the range of molecular vibrational modes (few tenths of eV), as this turns out to be the case for many species. In this mechanism, Z_{eff} is proportional to the density of molecular vibrational spectrum, which can be very large in polyatomics (see Sect. 2.2).

2.1 Direct annihilation

To understand the origin and size of enhancement in direct annihilation, consider the total wavefunction in the form (4). The second term in the square brackets represents the positron scattered wave. At low positron momenta, $kR \ll 1$, where R is the mean radius of the target, the scattering is dominated by the zero positron angular momentum and $f_{\mathbf{kk'}}$ can be replaced by the s-wave scattering amplitude f_0. It is known that f_0 can exceed the geometrical size of the target ($|f_0| \gg R$) when the system has a weakly bound or virtual level [37]. In this case, the wavefunction is enhanced in the vicinity of the target, leading to enhanced annihilation rates [23,32].

To evaluate the corresponding Z_{eff}, note that in the integral (3) the positron coordinate $\mathbf{r}$ is at or inside the target, i.e., where the electrons are. Nonetheless, one can use equation (4) to estimate Z_{eff} by assuming that positrons annihilate on the surface surrounding the target atom or molecule[4]. Hence, one obtains

$$Z_{eff}^{(dir)} \simeq 4\pi\rho_e \delta R |f_0|^2, \qquad (5)$$

where ρ_e is the electron density in the annihilation range (possibly enhanced by short-range electron-positron correlations), and δR is the range of distances where the positron annihilates [26]. Note that at low momenta the elastic cross section is also dominated by the s-wave contribution, $\sigma_{el} \simeq 4\pi|f_0|^2$. Hence, for $|f_0| \gg R$, both Z_{eff} and σ_{el} are enhanced.

Equation (5) allows one to estimate Z_{eff} due to direct annihilation. The factor $4\pi\rho_e\delta R \equiv F$ in (5) should be close to unity in atomic units[5]. At low momenta the scattering

---

[3] To date, quantum-chemistry calculations of positron binding have only been done for strongly polar molecules, where binding is guaranteed by the long-range dipole interaction, see, e.g., reference [36] and references therein.

[4] In fact, strong repulsion from the nuclei does prevent the positron from penetrating deep into the target.

[5] For example, for the simplest electron-positron bound system, positronium, in the ground state, $Ps(1s)$, $\rho_e \sim \rho_{Ps} = 1/8\pi$ a.u., and using $\delta R \sim 1$ a.u. one has $F \sim 0.5$ a.u.

amplitude can be written as $f_0 = -1/(\kappa + ik)$, where the small parameter κ is related to the energy of the virtual ($\kappa < 0$) or bound ($\kappa > 0$) state, $\varepsilon_0 = \pm \kappa^2/2$ [37]. Hence, $Z_{\text{eff}}^{(\text{dir})}$ is given by

$$Z_{\text{eff}}^{(\text{dir})} \simeq \frac{F}{\kappa^2 + k^2}. \qquad (6)$$

This equation shows that at zero positron energy $Z_{\text{eff}}^{(\text{dir})}$ can be made arbitrarily large by choosing ever smaller κ. However, for finite momenta the maximal possible values of $Z_{\text{eff}}^{(\text{dir})}$ are limited, e.g., for room temperature positrons, $k \sim 0.05$ a.u.,

$$Z_{\text{eff}}^{(\text{dir})} \lesssim 10^3. \qquad (7)$$

This means that relatively large values of Z_{eff} can still be understood in terms of the direct annihilation mechanism enhanced by the presence of a low-lying virtual or weakly-bound positron state. In particular, this explains thermal $Z_{\text{eff}} = 26.7$, 65.7 and 401 observed for the heavier noble gases, Ar, Kr and Xe, respectively [32,33]. On the other hand, explaining room-temperature values of $Z_{\text{eff}} > 10^3$ requires a different mechanism.

If the positron forms a bound state with the target, its total wavefunction, for the positron outside the target, can be written similarly to equation (4), as

$$\Psi_0(\mathbf{r}_1, \ldots, \mathbf{r}_Z, \mathbf{r}) \simeq \Phi_0(\mathbf{r}_1, \ldots, \mathbf{r}_Z) \frac{A}{r} e^{-\kappa r}, \qquad (8)$$

where A is the asymptotic normalisation constant. For a weakly bound state ($\kappa R \ll 1$) the positron exponent in (8) is very diffuse. The main contribution to the normalisation integral $\int |\Psi_0|^2 d\mathbf{r}_1 \ldots d\mathbf{r}_Z d\mathbf{r} = 1$, comes from large positron distances where (8) is valid, which yields $A = \sqrt{\kappa/2\pi}$. Hence, we can estimate the annihilation rate in the bound state (cf. Eqs. (2) and (3)),

$$\Gamma^a = \pi r_0^2 c \int \sum_{i=1}^{Z} \delta(\mathbf{r} - \mathbf{r}_i) |\Psi_0(\mathbf{r}_1, \ldots, \mathbf{r}_Z, \mathbf{r})|^2 d\mathbf{r}_1 \ldots d\mathbf{r}_Z d\mathbf{r} , \qquad (9)$$

using equation (8) in a way similar to the above estimate of $Z_{\text{eff}}^{(\text{dir})}$:

$$\Gamma^a \simeq \pi r_0^2 c \, 4\pi \rho_e \delta R |A|^2 = \pi r_0^2 c F \frac{\kappa}{2\pi}. \qquad (10)$$

This equation shows that Γ^a is proportional to κ, i.e., positron states with larger binding energies have greater annihilation rates [27,38]. A fit of the annihilation rates for a number of positron-atom bound states by equation (10) confirms this dependence and yields $F \approx 0.66$ a.u. [27].

2.2 Resonant annihilation

Resonant annihilation occurs in molecules capable of binding the positron. To be captured into a bound state, the positron energy must be absorbed by a vibrational excitation of the positron-molecule complex. This gives rise to

a VFR at the incident positron energy $\varepsilon = E_\nu + \varepsilon_0$, where E_ν is the vibrational excitation energy of the complex, and $\varepsilon_0 < 0$ is the positron bound state energy.

The resonant contribution to the annihilation cross section can be written using the Breit-Wigner formalism as a sum over the resonances [27,28,37],

$$\sigma_a = \frac{\pi}{k^2} \sum_\nu \frac{g_\nu \Gamma_\nu^a \Gamma_\nu^e}{(\varepsilon - E_\nu - \varepsilon_0)^2 + \frac{1}{4}\Gamma_\nu^2}, \qquad (11)$$

where Γ_ν^a, Γ_ν^e, and Γ_ν are the annihilation, elastic and total widths of νth resonance, and g_ν is its degeneracy. The annihilation width is proportional to the electron-positron contact density ρ_{ep} in the positron bound state and is practically independent of the vibrational excitation, $\Gamma_\nu^a = \Gamma^a = \pi r_0^2 c \rho_{ep}$, where $\rho_{ep} \simeq (F/2\pi)\kappa$ for a weakly bound state, cf. equations (9) and (10). Besides annihilation and elastic escape, the total width, $\Gamma_\nu = \Gamma_\nu^a + \Gamma_\nu^e + \Gamma_\nu^i$, may contain the contribution of positron inelastic escape, Γ_ν^i, i.e., that accompanied by vibrational excitation of the target, allowed for all vibrational excitations with energies below the incident positron energy $\varepsilon = k^2/2$.

From equations (2) and (11), the resonant Z_{eff} is given by

$$Z_{\text{eff}}^{(\text{res})} = \frac{\pi}{k} \rho_{ep} \sum_\nu \frac{g_\nu \Gamma_\nu^e}{(\varepsilon - E_\nu - \varepsilon_0)^2 + \frac{1}{4}\Gamma_\nu^2}. \qquad (12)$$

This equation can be compared directly with experiment if one knows the energies and widths of the resonances. To date, this has only been possible for a number of small polyatomics, namely methyl halides, methanol [39,40] and ethanol [41]. In these molecules all vibrational modes are infrared active, which enables one to evaluate their elastic widths using the dipole approximation. In methyl halides one can further assume that only mode-based VFR contribute to the sum in equation (12), and use $E_\nu = \omega_\nu$, where ω_ν are the mode frequencies. The only free parameter in this theory is the positron binding energy $|\varepsilon_0|$, which determines the downshift of the resonances, and affects the magnitude of $Z_{\text{eff}}^{(\text{res})}$ through $\rho_{ep} \propto \kappa$. Averaging $Z_{\text{eff}}^{(\text{res})}$ over the positron beam energy distribution and choosing ε_0 to fit the measured Z_{eff}, one obtains a very good agreement with experiment for CH_3F, CH_3Cl, and CH_3Br [39]. Theory can then make predictions for their deuterated analogs, which are expected to have the same binding energies [40].

The number of vibrational modes in a molecule is $3N - 6$, where N is the number of atoms. Hence, the contribution of mode-based VFR to Z_{eff} increases linearly with the size of the molecule. Experimental Z_{eff} show a much faster increase, see, e.g., Table 1. This means that in large polyatomics positron capture leads to excitation of vibrational combinations and overtones. Due to large vibrational spectrum densities, the spacing between the multimode VFRs is much smaller than the positron energy spread. This means that equation (12) must be averaged over an energy interval containing many such resonances. This yields

$$Z_{\text{eff}} = \frac{2\pi^2 \rho_{ep}}{k} \frac{\Gamma^e(\varepsilon)}{\Gamma(\varepsilon)} \rho(\varepsilon + |\varepsilon_0|), \qquad (13)$$

where $\Gamma^e(\varepsilon)$ and $\Gamma(\varepsilon)$ are the average elastic and total widths at the energy ε and $\rho(\varepsilon + |\varepsilon_0|)$ is the total level density of the positron-molecule vibrational excitations. Note that from now on we omit the superscript "(res)" from Z_{eff}, since for the molecules of interest, the resonant contribution is much greater than the direct one.

Using equation (9), one can check that the annihilation widths are very small, e.g., for a binding energy of 0.1 eV one obtains $\Gamma^a \sim 0.3$ μeV. The elastic width is determined by positron coupling to molecular vibrations. Assuming that it is greater than Γ^a (which is true at least for some small polyatomics, such as methyl halides [39]), and neglecting inelastic escape, one has $\Gamma \approx \Gamma^e$. After this equation (13) yields a simple estimate:

$$Z_{\text{eff}} \approx \frac{2\pi^2 \rho_{ep}}{k} \rho(\varepsilon + |\varepsilon_0|). \tag{14}$$

In this approximation the resonant contribution to Z_{eff} is basically determined by the vibrational spectrum density of the molecule [26,27].

The total vibrational density is easy to compute in the harmonic approximation, $E_\nu = \sum_k n_k \omega_k$, where the sum is over the modes, n_k are non-negative integers, and ω_k are the molecular mode frequencies[6]. For many species the latter are known from experiment [42], or can be evaluated by quantum chemistry packages, such as Q-Chem [43]. However, equation (14) predicts a much faster growth of Z_{eff} with molecular size [28] than that seen in Table 1, as the density increases sharply with the number of vibrational degrees of freedom. Consequently, the assumption that $\Gamma^e/\Gamma \approx 1$ is incorrect for such polyatomics, and we have $\Gamma^e/\Gamma \ll 1$. This can have two possible physical explanations. First, positrons may have a very weak coupling to multimode VFR, making their elastic widths small compared to the annihilation width, $\Gamma^e \ll \Gamma^a$. Such resonances will then be effectively decoupled from the positron continuum. Alternatively, the ratio Γ^e/Γ can be suppressed for multimode VFRs because of the contribution of vibrationally inelastic escape channels to Γ.

Let us evaluate the latter effect first. Here we also take into account that the target molecule may be in an excited initial state. For a molecule with initial vibrational energy E_v, the number of open vibrational positron escape channels is $N(\varepsilon + E_v) = \int_0^{\varepsilon + E_v} \rho(E) dE$. If the partial width associated with each of these channels is comparable to Γ^e, one will have $\Gamma^e/\Gamma \approx 1/N(\varepsilon + E_v)$, giving the following approximation for equation (13):

$$Z_{\text{eff}} \approx \frac{2\pi^2 \rho_{ep}}{k} \frac{\rho(\varepsilon + E_v + |\varepsilon_0|)}{N(\varepsilon + E_v)}. \tag{15}$$

For a given molecule this expression contains only one free parameter, namely, the positron binding energy $|\varepsilon_0|$. We average equation (15) over the initial target states with Boltzmann weights $\exp(-E_v/k_B T)$ and Maxwellian

---

[6] We assume that the vibrational spectrum of the weakly bound positron-molecule complex is the same as that of the neutral molecule.
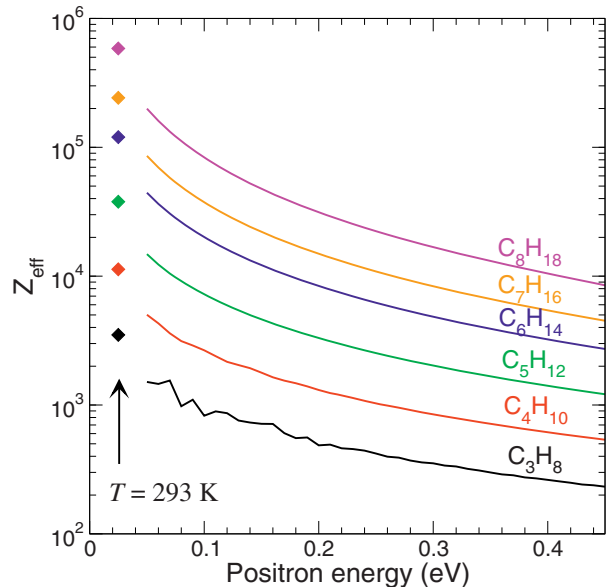

Fig. 1. (Color online) Experimental Z_{eff} measured with thermal positrons at room temperature (diamonds, values in Tab. 1) and calculated as a function of positron energy from equation (15) (solid curves), using ε_0 as an adjustable parameter to reproduce thermal Z_{eff}.

positron energy distribution, and choose $|\varepsilon_0|$ to reproduce experimental room-temperature Z_{eff} for alkanes with 3–8 carbons[7]. The corresponding estimates of the binding energies are given in Table 1. They are in good overall agreement with those inferred from the energy-resolved studies of Z_{eff} (see below).

With ε_0 values thus fixed, equation (15) can be used to predict the dependence of Z_{eff} on the positron energy for room-T targets. It produces fairly unremarkable curves shown in Figure 1. Their monotonic decrease is directly related to the rapid increase of $N(\varepsilon + E_v)$ in the denominator of equation (15).

As mentioned above, most of the experimental progress in recent years has been due a trap-based positron beam with a narrow ($\sim$25 meV) energy spread, built by the group of Surko at UCSD [44]. This development truly revolutionised positron annihilation studies by enabling energy-resolved measurements of Z_{eff}. Among the first results was the observation of a striking resonant structure in Z_{eff} shown in Figure 2, in sharp contrast with the predictions of equation (15).

Experimentalists immediately identified the prominent high-energy peak with resonant excitation of the C–H stretch modes [19], whose frequency in the alkanes is 0.37 eV. Its systematic downshift, seen clearly in Figure 2, is the measure of the positron-molecule binding energy which increases with molecular size (Tab. 1, last

---

[7] The frequencies of lowest carbon backbone modes for heavier alkanes obtained from Q-Chem contain large uncertainties.
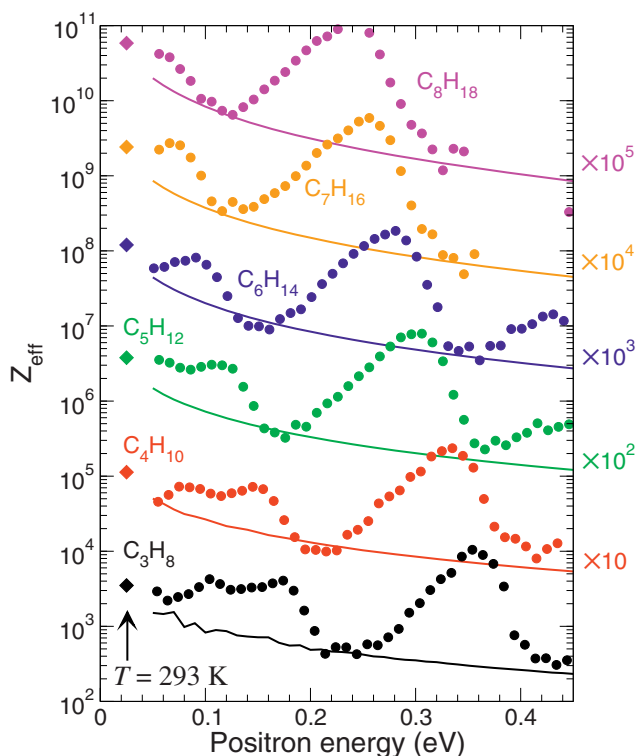
Fig. 2. (Color online) Experimental Z_{eff} measured with thermal positrons at room temperature (diamonds, values in Tab. 1) and calculated as a function of positron energy from equation (15) (solid curves), using ε_0 as an adjustable parameter to reproduce thermal Z_{eff}. Solid circles show Z_{eff} measured as a function of positron energy [19,20]. For the alkanes larger than butane, Z_{eff} have been multiplied by powers of 10 for clarity.

column). Figure 2 makes it obvious that the simple model which assumes that all (elastic and inelastic) vibrational escape widths are comparable, equation (15), is incorrect. Nonetheless, it produces meaningful binding energies for alkanes and yields Z_{eff} that scale correctly with molecular size.

A careful comparison of energy-resolved and thermal annihilation data was performed in reference [22]. It used the fact that $Z_{eff} \propto \sqrt{|\varepsilon_0|/\varepsilon}$, and proved that the energy-resolved Z_{eff} are in close agreement with the earlier thermal measurements. This confirms that all enhanced Z_{eff} in polatomics have a common vibrational origin. Experiment also provides indirect evidence against the importance of inelastic escape in alkanes [22,45]. They contrast with molecules in which one or two hydrogens are replaced by fluorines, and which likely show significant inelastic escape via excitation of the C–F stretch mode. Overall, our current understanding of the vibrational dynamics in positron-molecule complexes is at best incomplete.

3 Vibrational Feshbach resonances and doorways

As we have seen above, the energy dependence of enhanced Z_{eff} in polyatomics displays resonant structures that correlate with the spectra of fundamental vibrations [20–22]. Besides the prominent C–H stretch peak, lower-energy peaks can be identified with softer modes, i.e., bending and others. The vibrational nature of the peaks is further elucidated by studies of deuterated molecules [19,20,22,45]. Their electronic properties are nearly identical to those of the protonated ones. In particular, the positron binding energy of the protonated and deuterated species are very close. On the other hand, a factor of two change in the hydrogen nucleus mass changes the vibrational mode frequencies by up to 1.4 times (square root of the C–H bond reduced mass ratio). This results in a characteristic scaling of the energies of the resonant peaks, additional to the downshifts due to binding.

By examining peak shifts and using deuterated species as an extra check when needed, experimentalists have now established positron binding energies for over 20 molecules. Their values range from ~1 meV for small polyatomics, such as CH_3F and methanol, to tens of meV for heavier methyl halides and ethanol [21,39–41] and alkanes with 3–4 carbons, to 150 meV for benzene and 175 meV for chlorohexane, to 300 and 310 meV for naphthalene and hexadecane, respectively [22]. Experimentalists also identified additional Z_{eff} peaks in dodecane and heavier alkanes, which they ascribed to positronically-excited bound states (see Sect. 4).

While extremely useful and informative, the observed resonant structure in Z_{eff} also poses a serious question. The energy dependence of Z_{eff} looks as though the positron is captured by simple VFRs involving the fundamentals. On the other hand, the magnitude of Z_{eff} increases much faster than the number of modes, $3N - 6$. This can only be explained by assuming that positron capture is accompanied by multimode vibrational excitations, leading to a much larger density of VFR. Observations of the mode-like energy dependence and fast growth of Z_{eff} can be reconciled in a two-step model of positron capture, which involves the idea of mode-based vibrational *doorway* resonances [28]. This term originates from nuclear physics, where it means 'a metastable state formed in the initial state of the reaction', which 'may decay partly into the open channels (direct reactions), and partly through the coupling to the internal degrees of freedom' [46].

In this scheme, the positron first forms a bound state with the molecule, by transferring its excess energy to a near-resonant fundamental with energy $\omega_n \approx \varepsilon - \varepsilon_0$. This simple *doorway* state of the positron-molecule complex is embedded in the dense spectrum of multimode vibrations. Due to vibrational state mixing caused by anharmonic corrections (e.g., the anharmonicity of the molecular potential energy surface), the doorway state then decays or

"spreads" into multimode vibrational states[8]. Such decay takes place on a time scale $\tau \sim 1/\Gamma_{\rm spr}$, where $\Gamma_{\rm spr}$ is known as the spreading width.

To link the multimode VFR and doorway state resonance pictures together, consider the golden-rule perturbative expression for the positron elastic width,

$$\Gamma_\nu^e = 2\pi|\langle\Psi_\nu|V|0,\varepsilon\rangle|^2, \qquad (16)$$

where $|0,\varepsilon\rangle$ describes positron incident on the ground-state molecule, and V is the coupling between the incident positron and excited multimode eigenstate of the positron-molecule complex, $|\Psi_\nu\rangle$. The latter can be written as a linear combination

$$|\Psi_\nu\rangle = \sum_i C_i^{(\nu)}|\Phi_i\rangle, \qquad (17)$$

of some *harmonic* vibrational basis states $|\Phi_i\rangle$.

Let us assume that of all $|\Phi_i\rangle$, only those which describe 'bound positron + single-mode excitation', $|n,\varepsilon_0\rangle$, where n indicates the mode, are coupled to $|0,\varepsilon\rangle$. The coefficients $C_i^{(\nu)}$ describe mixing of this state with the multimode eigenstates ν (i.e., its spreading), and can be approximated by a Breit-Wigner shape,

$$|C_i^{(\nu)}|^2 \propto \frac{\Gamma_{\rm spr}^2/4}{(E_\nu - E_i)^2 + \Gamma_{\rm spr}^2/4}, \qquad (18)$$

subject to normalisation $\sum_i |C_i^{(\nu)}|^2 = 1$. Here E_ν and E_i are the energies of the eigen- and basis states, respectively, and $E_i = \omega_n + \varepsilon_0$ for $|\Phi_i\rangle = |n,\varepsilon_0\rangle$.

Using equations (13), (16), (17) and (18) (see [48] for the details of a similar derivation), one obtains $Z_{\rm eff}$ averaged over the energy on the scale of closely spaced VFRs,

$$Z_{\rm eff} = \frac{2\pi^2\rho_{ep}}{k}\frac{\Gamma_{\rm spr}}{2\pi\Gamma(\varepsilon)}\sum_n \frac{\Gamma_n^e}{(\varepsilon - \omega_n - \varepsilon_0)^2 + \frac{1}{4}\Gamma_{\rm spr}^2}, \quad (19)$$

where $\Gamma_n^e = 2\pi|\langle n,\varepsilon_0|V|0,\varepsilon\rangle|^2$. Note that equation (19) has the same structure as the original Breit-Wigner formula (12), except that (19) contains the elastic widths of the mode-based doorways, Γ_n^e, and the sum is over the *modes*.

Each of the Breit-Wigner profiles in (19) has a unit area, and for small $\Gamma_{\rm spr}$, is equivalent to a δ-function,

$$\frac{1}{2\pi}\frac{\Gamma_{\rm spr}}{(\varepsilon - \omega_n - \varepsilon_0)^2 + \frac{1}{4}\Gamma_{\rm spr}^2} \simeq \delta(\varepsilon - \omega_n - \varepsilon_0).$$

To compare with experiment, the delta-peaks must be convolved with the positron beam energy distribution, which determines the observed shapes of the resonances [39]. The integral contribution of each mode in equation (19)

Fig. 3. (Color online) Experimental $Z_{\rm eff}$ for butane, C_4H_{10} (solid circles) and octane, C_8H_{18} (scaled by a factor $1/50$, open circles) [20], compared with equation (19) folded with the positron beam energy distribution [39] for $\Gamma_{\rm spr} \ll 25$ meV. The fit for butane uses $|\varepsilon_0| = 35$ meV, $\Gamma_n^e/\Gamma = 7.2$ for C–H stretch modes and $\Gamma_n^e/\Gamma = 1.2$ for the rest; for octane, $|\varepsilon_0| = 122$ meV, $\Gamma_n^e/\Gamma = 84$ for C–H stretch modes and $\Gamma_n^e/\Gamma = 14$ for the rest.

is proportional to the ratio $\Gamma_n^e/\Gamma(\varepsilon)$. In contrast, the sum in equation (12) is over the true VFRs. Their density is much greater than that of the modes, but the contribution of each resonances, determined by Γ_ν^e/Γ_ν, is much smaller. This is due to the fact that each VFR carries only a small fraction of the elastic doorway width, $\Gamma_\nu^e \ll \Gamma_n^e$.

Besides explaining the energy dependence of $Z_{\rm eff}$ as due to the mode-based doorways, equation (19) also provides a new explanation of the enhanced $Z_{\rm eff}$ values. The latter are determined by three factors. With the increase of molecular size, the electron-positron contact density increases with the positron binding energy as $\rho_{ep} \propto |\varepsilon_0|^{1/2}$. Experiment shows that for alkanes $|\varepsilon_0|$ grows approximately linearly, by 20 meV per monomer. The number of terms in the sum (19) increases as the number of vibrational degrees of freedom, i.e., linearly. The rest of the enhancement comes from a *suppression* of the total width $\Gamma(\varepsilon)$. Since the annihilation widths grows with ρ_{ep}, the latter is only possible if $\Gamma^a \ll \Gamma$. We therefore see that the total width must be dominated by vibrationally elastic and inelastic escape[9]. When Γ becomes comparable to Γ^a for very large molecules, the rapid growth of $Z_{\rm eff}$ saturates [22].

To illustrate the applicability of equation (19), we use it to fit the experimental data for butane and octane [20], as shown in Figure 3. This is done by convolving the narrow resonant peaks with the positron beam energy distribution, see reference [39]. We use $|\varepsilon_0| = 35$ and 122 meV,

---

[8] This process is usually termed intramolecular vibrational energy redistribution (IVR). This is one of the paradigms of molecular reaction theories, that has been probed experimentally by other means, e.g., fluorescence [47].
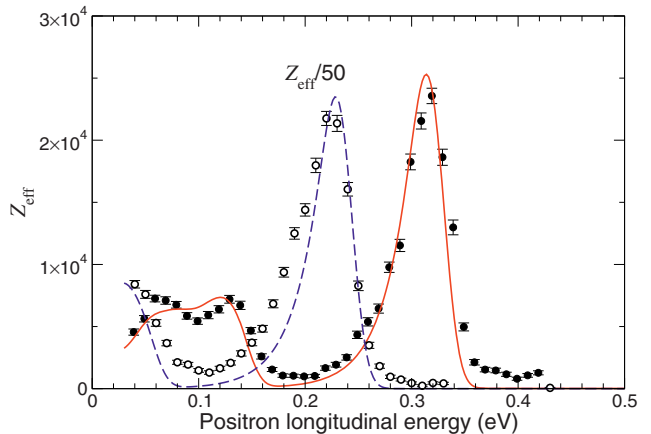
[9] Evidence based on VFR of the second positronically excited bound state and some other trends in molecular $Z_{\rm eff}$ appear to speak against vibrationally-inelastic escape [22]. However, singly- and doubly-fluorinated alkane provide striking evidence of the importance of this process which leads to a strong suppression of the C–H peak.

for the binding energies of the two species. The remaining unknown parameter is the ratio $\Gamma_n^e/\Gamma(\varepsilon)$. Given the difference between the C–H stretch and low-energy mode peaks, we use two values for these groups of modes, the former six times greater than the latter (see caption of Fig. 3). The ratios Γ_n^e/Γ for octane, whose Z_{eff} is about 50 time greater than that of butane, are approximately 12 times larger than for butane. This reflects a greater degree of mixing between multimode VFR in the larger molecule.

Concluding this section, we must emphasize that in spite of the good look of the fits in Figure 3, the details of IVR that accompanies positron capture remain unclear. The amount of vibrational energy transferred to the molecule in this process can be quite low (e.g., for thermal 300 K positrons). However, room-temperature Z_{eff} and their values at the vibrational peaks are in complete accord [22]. In principle, for large molecules one may also need to take into account their significant thermal energy content. The only data available to date are for pentane and heptane [49]. In these molecules lowering the gas temperature by a factor of two results in a small growth of Z_{eff} at low positron energy and almost no change at the C–H peak. We hope that the information contained in the positron annihilation signal will soon allow one to understand such details. No doubt, this would be useful for a better understanding of similar processes for electron-induced VFRs [50].

4 Positron binding

In Section 2.2 we used thermal Z_{eff} to obtain estimates of the positron binding energies for alkanes, and compared them with the values found experimentally (Tab. 1). In fact, nearly all information on positron-molecule binding comes from the energy-resolved Z_{eff} measurements.

Calculation of positron binding is a nontrivial task. The electrostatic interaction between positrons and neutral atoms or molecules (without large dipole moments) is dominated by nuclear repulsion. At large positron-target separations, the electric field of the positron polarises the neutral, which gives rise to the $-\alpha e^2/2r^4$ attractive potential, α being the atomic or molecular dipole polarisability. At short range, an additional interaction due virtual positronium formation, akin to covalent bonding, increases the overall attraction [34]. Together with polarisation, they overcome the static repulsion at low positron energies, and enable the formation of virtual levels or even bound states.

To describe the positron interaction with a neutral, one must be able to include both long- and short-range correlation effects. So far, reliable calculations of positron bound states have been done for about ten atoms [35] and a few strongly polar molecules [36]. Good-quality ab initio calculations of positron binding to alkanes and similar large molecules currently appear to be out of reach.

In this situation we proposed that the problem of binding can be usefully explored using zero-range potentials (ZRP) [51]. ZRP is probably the simplest form of a model
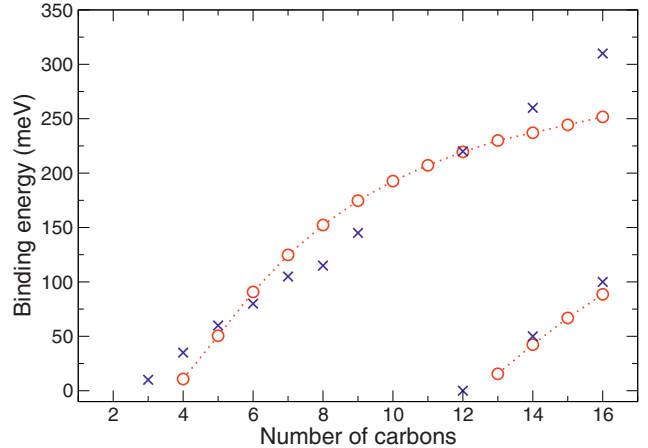

Fig. 4. (Color online) Positron binding energies for alkanes determined from experiment (crosses, see Tab. 1) and calculated using the ZRP model (circles). The parameter of the ZRP model is chosen to reproduce $\varepsilon_0 = -220$ meV for dodecane.

potential. It is especially suited for studying low-energy processes [52]. The main idea of a model potential approach is to fix the parameters of the interaction by comparison with experimental data, e.g., the binding energy of a given molecule, and then use this potential to study binding for a whole range of similar molecules.

In the ZRP method, the bound-state wavefunction of the positron in the field of N centres placed at $\mathbf{R}_i$ has the form [52],

$$\Psi = \sum_{i=1}^{N} A_i \frac{e^{-\kappa|\mathbf{r}-\mathbf{R}_i|}}{|\mathbf{r}-\mathbf{R}_i|}, \qquad (20)$$

where $\kappa > 0$ is related to the bound-state energy by $\varepsilon_0 = -\kappa^2/2$. The interaction with each centre is parametrised by κ_{0i}, through the boundary condition,

$$\Psi\mid_{\mathbf{r}\to\mathbf{R}_i} \simeq \text{const} \times \left(\frac{1}{|\mathbf{r}-\mathbf{R}_i|} - \kappa_{0i} \right). \qquad (21)$$

Subjecting Ψ from (20) to N conditions (21) yields a set of linear homogeneous equations for A_i, whose solvability determines the allowed values of κ.

We model alkanes, C_nH_{2n+2}, by a planar zig-zag chain of n ZRPs, each representing the CH_3 or CH_2 group. The distance between the neighbouring ZRPs is given by the length of the C–C bond, i.e., 2.911 a.u., and the angle between adjacent bonds is equal to 113°. We choose $\kappa_{0i} = -0.6915$ a.u. for all i, to reproduce the binding energy for dodecane ($n = 12$): $\varepsilon_0 = -220$ meV[10]. In Figure 4 the results of our calculations for all alkanes up to $n = 16$ are compared with the experimental binding energies inferred from the C–H peak shifts, Table 1.

---

[10] In reference [51] we used $\kappa_{0i} = -0.52$ a.u., to fit the binding energy of propane ($n = 3$), the smallest firmly established for alkanes. This resulted in a factor-of-two overestimation of the binding energies for all $n \geq 4$.

Figure 4 shows that the model gives a good overall description of binding, although it predicts that the system for $n = 3$ is unbound. The model predicts that a 2nd bound state emerges for $n = 13$, while the experiment observes this state for dodecane already [21,22]. This difference aside, the calculation gives an excellent description of the 2nd bound state energy.

To visualise the bound states, we calculate the two-dimensional density

$$\rho(x, y) = \int_{-\infty}^{+\infty} |\Psi(x, y, z)|^2 dz, \qquad (22)$$

where x and y are in the plane containing the carbon chain. The densities for the 1st and 2nd bound states in tetradecane ($n = 14$) are shown in Figure 5. Both states are quite diffuse, with the positron spread all over the molecule. Note that since the wavefunction of the 2nd bound state is orthogonal to that of the ground state, it changes sign somewhere on the surface separating the two ends of the molecule. On the density plot, this corresponds to an area of low density near the middle of the molecule.

5 Annihilation spectra and fragmentation

There are other important and interesting phenomena related to positron-molecule annihilation. Experiments with positrons in a trap enabled accurate measurements of the annihilation γ spectra for a large number of large polyatomics [53]. For low-energy positrons the Doppler broadening of the 511 keV line is mostly due to the velocity distribution of the bound electrons on which the positron annihilates. Hence, the shapes of the γ spectra can be used to characterise the electron orbitals involved. For example, annihilation with faster electrons in C–F bonds produces much broader spectra than annihilation with C–H electrons. Using this difference, experimentalists analysed the annihilation spectra of partially fluorinated hydrocarbons in terms of a linear combination of the C–F and C–H spectra, and deduced the fraction of annihilation events involving the fluorine electrons. An important conclusion of that study was that annihilation on any valence or near-valence electron is equally probable, i.e., that the positron wave function is not localised on any particular site of the molecule. (This could be expected when annihilation takes place in diffuse bound states, like those shown in Fig. 5.)

Another phenomenon is the ionisation and fragmentation of molecules following annihilation. It takes place when the positron energy is below the Ps-formation threshold[11]. The first study of this kind, reference [54],

[11] Positrons with energies $\varepsilon > I - |E_{1s}|$, where I is the ionisation potential of the molecule, and $E_{1s} = -6.8$ eV is the ground-state energy of Ps, can ionise molecules by forming Ps, which subsequently annihilates.
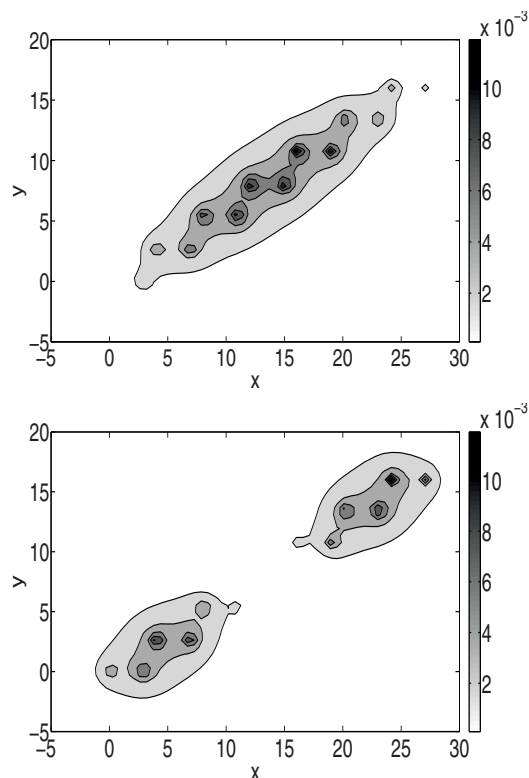

Fig. 5. Two-dimensional density of the positron wavefunctions in the ZRP model for the 1st (top) and 2nd (bottom) bound states in tetradecane. In the plots, the C–C bonds are alternately parallel and at $67°$ degrees to the x axis.

revealed that room-temperature positrons annihilating in alkane molecules produce a broad spectrum of fragment ions. Hulett and collaborators conducted detailed studies of many aspects of this phenomenon [55]. In particular, they showed that molecular fragmentation is strong far below and far above the Ps-formation threshold, but small just above it. The fragmentation patterns in the two regimes are also quite different. Hence, positrons could be used to selectively ionize and fragment ions, for example, in mass spectroscopic analysis.

A new possibility of inducing selective fragmentation is offered by the different positron density distributions in the 1st and 2nd bound states (Fig. 5). Annihilation in VFRs involving the positron ground state will remove electrons predominantly from the bonds around the centre of the molecule. This can favour near-equal-mass fragmentation. On the other hand, in the resonances involving positronically excited bound states, the electrons in the bonds near to the two extremes are likely to be annihilated. This can prompt a more asymmetric fragmentation. At present the only model of sub-Ps-threshold fragmentation is that developed by Crawford [56]. Its key element is the understanding that by annihilating with electrons in the lower valence orbitals, the positron can deposit substantial amounts of energy in the molecule.

6 Summary

Positron annihilation in molecules is a fascinating problem at the interface of quantum electrodynamics, atomic physics, chemistry, and medical and technological applications. Its main feature is the very large positron annihilation rates in many polyatomics such as alkanes and their substitutes[12]. It can be explained by positron capture into vibrational Feshbach resonances. At the physical level, such capture means that the positrons are held by the molecules for long periods of time, which enhances the annihilation probability.

A detailed understanding of the annihilation process requires calculations of positron binding and annihilation rates in the bound states, evaluation of the positron coupling to molecular vibrations, understanding the role of mode-based vibrational doorways, and their spreading into complex multimode vibrations (i.e., IVR). Some of these questions, such as IVR, are important in many other contexts, e.g., in chemical reactions and electron-molecule collisions. Viewing positron annihilation as a probe, one can hope that it will shed light on these problems too.

Finally, the abundance of positrons and diversity of their uses, from cosmic problems [9] to novel cancer treatment techniques, such as positherapy [3] make the positron annihilation problem relevant in many contiguous areas.

References

1. R.L. Wahl, J.W. Buchanan, *Principles and Practice of Positron Emission Tomography* (Lippincott, Williams and Wilkins, Philadelphia, 2002)
2. H. Müller, W. Enghardt, Phys. Med. Biol. **51**, 1779 (2006); I. Pshenichnov, I. Mishustin, W. Greiner, Phys. Med. Biol. **51**, 6099 (2006)
3. R.M. Moadel et al., Cancer Res. **65**, 698 (2005)
4. *Electron-Molecule Interactions and Their Applications*, edited by L.G. Christophorou (Academic Press, New York, 1984)
5. F. Martin, P.D. Burrow, Z. Cai, P. Cloutier, D. Hunting, L. Sanche, Phys. Rev. Lett. **93**, 068101 (2004)
6. P.A.M. Dirac, Proc. Roy. Soc. London **126**, 360 (1930)
7. C.D. Anderson, Phys. Rev. **43**, 491 (1933)
8. P.G. Coleman, *Positron Beams and Their Applications* (World Scientific, Singapore, 2000)
9. S. Sazonov, E. Churazov, R. Sunyaev, M. Revnivtsev, J. Exp. Astron. **20**, 15 (2005)
10. V.B. Berestetskii, E.M. Lifshitz, L.P. Pitaevskii, *Quantum Electrodynamics* (Pergamon, Oxford, 1982)
11. P.A. Fraser, Adv. At. Mol. Opt. Phys. **4**, 63 (1968)
12. M. Deutsch, Phys. Rev. **83**, 866 (1951)
13. D.A.L. Paul, L. Saint-Pierre, Phys. Rev. Lett. **11**, 493 (1963)
14. S.J. Tao, Phys. Rev. Lett. **14**, 935 (1965)
15. G.R. Heyland, M. Charlton, T.C. Griffith, G.L. Wright, Can. J. Phys. **60**, 503 (1982)
16. G.L. Wright, M. Charlton, T.C. Griffith, G.R. Heyland, J. Phys. B **18**, 4327 (1985)
17. C.M. Surko, A. Passner, M. Leventhal, F.J. Wysocki, Phys. Rev. Lett. **61**, 1831 (1988); T.J. Murphy, C.M. Surko, Phys. Rev. Lett. **67**, 2954 (1991)
18. K. Iwata, R.G. Greaves, T.J. Murphy, M.D. Tinkle, C.M. Surko, Phys. Rev. A **51**, 473 (1995)
19. S.J. Gilbert, L.D. Barnes, J.P. Sullivan, C.M. Surko, Phys. Rev. Lett. **88**, 043201 (2002)
20. L.D. Barnes, S.J. Gilbert, C.M. Surko, Phys. Rev. A **67**, 032706 (2003)
21. L.D. Barnes, J.A. Young, C.M. Surko, Phys. Rev. A **74**, 012706 (2006)
22. J.A. Young, C.M. Surko, Phys. Rev. A **77**, 052704 (2008)
23. V.I. Goldanskii, Yu.S. Sayasov, Phys. Lett. **13**, 300 (1964)
24. P.M. Smith, D.A.L. Paul, Can. J. Phys. **48**, 2984 (1970)
25. G.K. Ivanov, Dokl. Akad. Nauk SSSR **291**, 622 (1986), Dokl. Phys. Chem. **291**, 1048 (1986); Chem. Phys. Lett. **135**, 89 (1987)
26. G.F. Gribakin, Phys. Rev. A **61**, 022720 (2000)
27. G.F. Gribakin, in *New Directions in Antimatter Chemistry and Physics*, edited by C.M. Surko and F.A. Gianturco (Kluwer Academic Publishers, Netherlands, 2001), p. 413
28. G.F. Gribakin, P.M.W. Gill, Nucl. Instrum. Meth. B **221**, 30 (2004)
29. F.A. Gianturco, T. Mukherjee, A. Occhigrossi, Phys. Rev. A **64**, 032715 (2001); A. Occhigrossi, F.A. Gianturco, J. Phys. B **36**, 1383 (2003); J. Franz, F.A. Gianturco, Nucl. Instrum. Meth. B **247**, 20 (2006)
30. E.P. da Silva, J.S.E. Germano, M.A.P. Lima, Phys. Rev. A **49**, R1527 (1994); M.T. do N. Varella, C.R.C. de Carvalho, M.A.P. Lima, Nucl. Instrum. Meth. B **192**, 225 (2002)
31. T. Nishimura, F.A. Gianturco, Phys. Rev. Lett. **90**, 183201 (2003); Phys. Rev. A **72**, 022706 (2005)
32. V.A. Dzuba, V.V. Flambaum, W.A. King, B.N. Miller, O.P. Sushkov, Phys. Scr. T **46**, 248 (1993)
33. V.A. Dzuba, V.V. Flambaum, G.F. Gribakin, W.A. King, J. Phys. B **29**, 3151 (1996)
34. V.A. Dzuba, V.V. Flambaum, G.F. Gribakin, W.A. King, Phys. Rev. A **52**, 4541 (1995)
35. J. Mitroy, M.W.J. Bromley, G.G. Ryzhikh, J. Phys. B **35**, R81 (2002)
36. H. Chojnacki, K. Strasburger, Molec. Phys. **104**, 2273 (2006)
37. L.D. Landau, E.M. Lifshitz, *Quantum Mechanics*, 3rd edn. (Pergamon, Oxford, 1977)
38. J. Mitroy, I.A. Ivanov, Phys. Rev. A **65**, 042705 (2002)
39. G.F. Gribakin, C.M.R. Lee, Phys. Rev. Lett. **97**, 193201 (2006)

---

[12] Perfluorinated alkanes seem to be largely an exception. They have high ionisation potentials, as the fluorine atoms hold tightly to their electrons. This makes them fairly "unattractive" for the positron, and most likely incapable of binding. Therefore, resonant annihilation is switched off for them, which explains their relatively low Z_{eff} that grow slowly with molecular size.

40. J.A. Young, G.F. Gribakin, C.M.R. Lee, C.M. Surko, Phys. Rev. A **77**, 060702 (2008)

41. J.A. Young, C.M. Surko, Phys. Rev. A **78**, 032702 (2008)

42. NIST Chemistry WebBook, NIST Standard Reference Database Number 69, June 2005, edited by P.J. Linstrom, W.G. Mallard, `http://webbook.nist.gov/chemistry/`

43. J. Kong et al., J. Comput. Chem. **21**, 1532 (2000)

44. S.J. Gilbert, C. Kurz, R.G. Greaves, C.M. Surko, Appl. Phys. Lett. **70**, 1944 (1997)

45. J.A. Young, C.M. Surko, Phys. Rev. Lett. **99**, 133201 (2007)

46. A. Bohr, B. Mottelson, *Nuclear Structure*, Vol. 1 (World Scientific, Singapore, 1998), p. 434

47. G.M. Stewart, J.D. McDonald, J. Chem. Phys. **78**, 3907 (1983)

48. V.V. Flambaum, A.A. Gribakina, G.F. Gribakin, C. Harabati, Phys. Rev. A **66**, 012713 (2002)

49. J.A. Young, C.M. Surko, Nucl. Instrum. Meth. B **266**, 478 (2008)

50. H. Hotop, M.-W. Ruf, M. Allan, I.I. Fabrikant, Adv. At. Mol. Opt. Phys. **49**, 85 (2003)

51. G.F. Gribakin, C.M.R. Lee, Nucl. Instrum. Meth. B **247**, 31 (2006)

52. Yu.N. Demkov, V.N. Ostrovsky, *Zero-Range Potentials and their Applications in Atomic Physics* (Plenum Press, New York, 1988)

53. K. Iwata, R.G. Greaves, C.M. Surko, Phys. Rev. A **55**, 3586 (1997)

54. A. Passner, C.M. Surko, M. Leventhal, A.P. Mills, Jr. Phys. Rev. A **39**, 3706 (1989); G.L. Glish, R.G. Greaves, S.A. McLuckey, L.D. Hulett, C.M. Surko, J. Xu, D.L. Donohue, Phys. Rev. A **49**, 2389 (1994)

55. L.D. Hulett, D.L. Donohue, J. Xu, T.A. Lewis, S.A. McLuckey, G.L. Glish, Chem. Phys. Lett. **216**, 236 (1993); D.L. Donohue, L.D. Hulett, Jr., B.A. Eckenrode, S.A. McLuckey, G.L. Glish, Chem. Phys. Lett. **168**, 37 (1990); J. Xu, L.D. Hulett, Jr., T.A. Lewis, D.L. Donohue, S.A. McLuckey, G.L. Glish, Phys. Rev. A **47**, 1023 (1993); J. Xu, L.D. Hulett, T.A. Lewis, D.L. Donohue, S.A. McLuckey, O.H. Crawford, Phys. Rev. A **49**, R3151 (1994); J. Xu, L.D. Hulett, Jr., T.A. Lewis, S.A. McLuckey, Phys. Rev. A **52**, 2088 (1995); J. Moxom, D.M. Schrader, G. Laricchia, J. Xu, L.D. Hulett, Phys. Rev. A **62**, 052708 (2000)

56. O.H. Crawford, Phys. Rev. A **49**, R3147 (1994)